Far-infrared Observation of the Energy Gap in Au_{55} Nanoparticles

Johann Y. H. Kim and Xuandong Zhao

Department of Physics, University of Cincinnati, Cincinnati, Ohio 45221, U. S. A.

and

Günter Schmid

Universität Duisburg-Essen, Institut für Anorganische Chemie, Essen 45117, Germany

(Submitted October 27, 2010)

We have carried out the far-infrared (far-IR) transmission measurements on the ligand stabilized Au_{55} nanoparticles dispersed in Teflon at volume fractions ranging from 0.2% to 1%. We have observed a broad far-IR absorption with an onset at $\Delta \sim 10$ cm^{-1} that follows $\propto \sqrt{\omega - \Delta}$ instead of a series of peaks which might arise from the electron transition between discrete energy levels. This frequency dependence is totally unexpected and completely different from that of the absorption due to the induced electric dipole. The onset of the absorption reminiscent of an energy gap Δ at ~ 10 cm^{-1} ($\sim$ 1. 2 meV) is surprisingly smaller than that of the expected for a metal sphere of 5.3 Å in radius and independent of temperature. In this work we did not observe the level correlation effect in the absorption coefficient. It is concluded that Au_{55} nanoparticles behave like a semimetal with an energy gap $\Delta \sim 10$ cm^{-1} rather than a giant atom.

PACS Number: 78.30.-j, 78.67.-n, 78.67.Bf

Physics in the length scale of nanometer (10^{-9} m) is now at the center of focus in the research area of nanoscale electronic devices such as a single electron transistor and in molecular biological systems. [1] Among a variety of nanosystems, metal nanoparticles [2] are of special interest because free electrons are now confined to a length scale that is small enough to push the electrons into the realm of quantum mechanics yet large enough to retain the solid-state characteristics. In particular, chemical synthesis of metal nanoparticles without size distribution has opened a window of opportunity to understand the electronic properties of metal nanoparticles, which was not feasible due to the particle size distribution. In this work, we focus on an unobserved problem in condensed matter physics, namely far-infrared (far-IR) observation of the size-quantized energy gap in a metal nanoparticle.

Far-IR absorption study of metal nanoparticles was initially motivated by the possibility of observing transitions of electrons between discrete energy levels and quantum size effect on the induced electric dipole absorption properties of classical nanoparticles in oscillating uniform electric field. For disordered metal nanoparticles with surface roughness to atomic scale, the average energy gap at the Fermi energy (E_F) of a metal nanoparticle that contains N electrons would be $\boxed{\overline{\Delta} \approx E_F / N}$ which is known as Kubo gap [3]. In this picture, $\overline{\Delta}$ satisfies the Poisson distribution for an ensemble of metal nanoparticles. Gor'kov and Eliashberg (GE) [4] proposed that the randomness of the level distribution in an ensemble of metal nanoparticles of $\overline{\Delta}$ could be described by the statistical theory of levels (random matrix theory) [5, 6]. As a result, the GE model predicts oscillations in the far-IR absorption coefficient superimposed on a background which is proportional to ω^2. However, it was shown that this oscillation could be easily wiped out when the particle size distribution was considered [7]. Thus no evidence of level correlation effect has been obtained by a far-IR experiment.

In this work, we have carried out far-IR absorption measurements on the chemically synthesized, ligand-stabilized Au_{55} nanoparticles ($Au_{55}(PPh_3)_{12}Cl_6$) [8]. Studying $Au_{55}(PPh_3)_{12}Cl_6$ (Au55 hereafter) nanoparticles offers an unprecedented opportunity to address specific issues because the Au55 nanoparticles are monodispersed in size and their electrical isolation is guaranteed by the presence of the ligand molecules on each Au55 nanoparticle. As shown in Figure 1, the structure of Au55 can be modeled as the Au_{13} nanoparticle surrounded by the shell of 42 Au atoms. Among 42 outer Au atoms, there are 24 non-coordinated surface atoms and 6 Cl atoms are located in the center of 6 squares and 12 corner surface atoms coordinated with PPh_3 (PPh_3 = Triphenylphosphine) ligands. Thus each Au55 nanoparticle of diameter 14 Å is surrounded by PPh_3 molecules and Cl atoms, making the size of Au55 nanoparticle be 21 Å in diameter. Therefore, the distance between two Au55 nanoparticles in contact would be ~ 7 Å, hence, ensuring the electrical isolation between the particles. Therefore, the number of "free" electrons in Au55 may be estimated to be 13 + 24 = 37.

The radius of a classical Au sphere that contains 37 electrons would be 5.3 Å using the density of free electrons of Au, 5.90 x 10^{22} electrons/cm^3. Even if we take into account of the electron density depletion due to the electronegative 6 Cl atoms on the surface and the fact that Au-Au distance in the nanoparticle is slightly greater than that of the bulk Au, a ~ 5.3 Å is a reasonable estimate. Then the quantized energy levels may be calculated by solving the Schrödinger equation for a three-dimensional (3D) infinite potential well. Since the radial wave function $R_{n\ell}(r)$ is proportional to the spherical Bessel's function $j_\ell(kr)$ only, the value of k can be determined by imposing the boundary condition $j_\ell(ka) = 0$ at $r = a = 5.3$ Å. If we write the n^{th} zero of $j_\ell(z)$ as $z_{n\ell}$, the allowed energy levels are $E_{n\ell} = z_{n\ell}^2 \hbar^2 / 2ma^2 = 0.008\, z_{n\ell}^2$ eV where n =

1, 2, 3,… and ℓ = 0, 1, 2, … (n-1). The corresponding energy levels are depicted in the diagram shown in Figure 1.

For the far-IR absorption measurements, Au55 nanoparticles were dispersed in Teflon particle host (0.6 μm in diameter) at various volume fractions, f = 0.002, 0.004, 0.006, 0.008, and 0.01. The Au55 nanoparticle/Teflon mixture (Au55/Teflon) was ground at T = 77 K in order to ensure uniform distribution of Au55 nanoparticles in Teflon matrix. Then the Au55/Teflon mixture was compressed into a 1 cm diameter pellet at 20,000 psi. The pellet thickness was maintained at around ~ 5 mm in order to avoid the interference fringes in the far-IR transmission spectra due to the multiple interference between the front and back surfaces. The far-IR transmission measurements were done using a Bruker 113v spectrometer with a Si-composite bolometer detector normally operating at 4.2 K. In order to cover the frequency below 20 cm^{-1}, a 75 μm Mylar beam splitter and a doped-Si-composite bolometer with 1 cm^2 active area operating at 2 K in conjunction with a parabolic light cone with a 7 mm diameter exit aperture were used.

Typical far-IR transmission data as taken (raw data) at various temperatures for f = 0.01 sample using three different Mylar beam splitters (75 μm, 23 μm, and 12 μm) are displayed in Figure 2. Two things are clear: (1) The transmission is independent of temperature [9] and (2) there appears a gap-like feature at ~ 10 cm^{-1}. In addition there appear vibration modes of $(-CF_2-CF_2-)_n$ (Teflon) at T_0 = 52 cm^{-1} and T_3 mode at 72 cm^{-1}. The T_0 mode at T = 300 K, which is the z-axis rotation of free molecule in Teflon unit cell, appears to split into two peaks T_1 at 43 cm^{-1} and T_2 at 52 cm^{-1} at low temperature (see the inset of Figure 2) which is due to the in-phase and out-of-phase coupling that occurs in the unit cell of low temperature phase [10]. The T_3 mode is then one of the three translational lattice modes. There also appears an intense absorption at ~ 200 cm^{-1} which is the CF_2 twisting mode in Teflon [10].

The absorption coefficient of Au55/Teflon composite pellet of thickness d was calculated from transmission (T) via $\alpha(\omega) = -\ln(T)/d + 2\ln(1-R)/d$. Here R is the far-IR reflectivity of the sample. Therefore we find α_{Au55} from $\alpha_{Au55} = \alpha_{Au55/Teflon} - \alpha_{Teflon}$ by assuming that $R_{Au55/Teflon} \approx R_{Teflon}$ at such dilute Au55 nanoparticle concentration. α_{Au55} for f=0.01 measured at T = 10 K is displayed in Figure 3. For comparison, an absorption graph of pure PPh_3 ligand molecule (f = 0.01) is also displayed. Since the ligand compound contains only phenyl and phophorus, the ligand part is expected to be transparent in the far-IR and, therefore, the frequency dependence of α_{Au55} will not be affected by the presence of the ligand shell as shown in Figure 3 except for the vibrations indicated as L_1 and L_2 which commonly present in both Au55 and the ligand molecule. Notice that the T_3 mode of the Teflon has not been fully compensated by the subtraction because it has greater oscillator strength in Au55/Teflon composite than in pure Teflon. The sharp upturn in the vicinity of 170 cm^{-1} is also due to incomplete subtraction of the intense ~ 200 cm^{-1} mode in Teflon. The α_{Au55}/f plot for f = 0.002, 0.004, 0.006, 0.008, and 0.01 samples shown in the inset of Figure 3 demonstrates that the absorption is linear in f and, hence, excluding a possibility of inter-particle electron tunneling which would result a non-linear f dependence. Furthermore since the energy required to add an electron to a nanoparticle ($e^2/2C$ with $C = 4\pi\varepsilon_0 a$) is in the range of ~ 0.5 eV for Au55, inter-particle tunneling is not likely under the far-IR experimental conditions.

For a classical Au nanoparticle of radius a, σ_1 may be written as $\sigma_1 = 5.94a$ $\Omega^{-1}cm^{-1}$ with a in Å and the Fermi velocity for Au v_F = 1.4 x 10^{10} cm/s by expressing the scattering rate as $\Gamma = a/v_F$ since a is much smaller than electron mean-free-path of Au. Then the corresponding absorption takes the form $\alpha_{Au} = 0.159 f \nu^2/a$ where $\nu = \omega/2\pi c$ [11]. α_{Au} for a = 5.3 Å classical Au nanoparticle at f = 0.01 is shown in Figure 4 along with the absorption graphs of f = 0.01

Au55. It is important to note first that the frequency dependence of α_{Au55} is completely different from that of classical nanoparticles ($\propto \nu^2$), suggesting that the origin of far-IR absorption by Au55 is not in the electric dipole absorption. Notice also that instead of a series of sharp peaks as seen in the STM study of a Au55 nanoparticle [12], the far-IR absorption spectrum has a broad background absorption that resembles the shape of the 3D joint-density of states ($\propto \sqrt{\omega - \Delta}$) with a gap Δ at ~ 10 cm^{-1} (1.2 meV).

For 37 electrons in the 3D square well potential, the highest occupied energy level would be $E_{n\ell} = E_{21} = 0.477$ eV which has six-fold degeneracy. Then the first few dominant allowed transitions $(\Delta\ell = \pm 1)$ are $\hbar\omega_1 = E_{14} - E_{13} = 0.145\, eV$, $\hbar\omega_2 = E_{22} - E_{21} = 0.185\, eV$, and $\hbar\omega_3 = E_{22} - E_{13} = 0.271\, eV$, which are far larger than the observed. Since the boundary for the electrons in Au55 particles is expected to be rough to atomic scale and its shape is not a sphere, all the degeneracy may be lifted. If the energy levels are completely random as in a disordered metal particle, we have the Kubo gap $\overline{\Delta} \approx E_F / N \approx 0.149\, eV$.

Based on the discussions above, such a small far-IR energy gap seen at ~ 1.2 meV is unexpected. However, in the above single particle picture, we have not considered the Coulomb interactions between the electrons. Since we anticipate poor screening of the Coulomb interactions in Au55 unlike in the bulk where the Coulomb interaction between the electrons is effectively screened out. Therefore considering the Coulomb energies in the doubly occupied state (U_0) and in the singly occupied state (U_1), we may reconcile the discrepancy between the far-IR energy gap and the tunneling gap. In this picture the Coulomb energy difference $U_1 - U_0$ may be estimated by calculating the amount of red-shift in Δ from the expected energy gap $\overline{\Delta} \approx 0.149\, eV$. Using Δ ~ 10 cm^{-1} = 1.2 meV, we find $U_1 - U_0 \approx -0.148\, eV$. Since the electron tunneling spectroscopy is not subjected to the dipole selection rules and to the Coulomb energy

difference, more or so evenly spaced tunneling spectra with energy comparable to $\overline{\Delta} \approx 0.15\, eV$ should be seen [12]. Yi and Sheng [13] found that including the Coulomb interactions and the Breit interaction substantially lowers $\overline{\Delta}$. However, a rigorously calculation of the Coulomb correlation energy difference in optical transitions remains to be seen.

It is surprising to see the absence of any oscillatory behavior in the absorption spectrum that may arise from the energy level correlation in the ensemble of Au55 nanoparticles. In addition the far-IR absorption is independent of magnetic field up to 14 Tesla [14]. Furthermore we found the far-IR absorption $\propto \sqrt{\omega - \Delta}$ with $\Delta \sim 1.2$ meV. This behavior may be understood by giving quantum mechanical consideration as $\alpha(\omega) \sim \sum_{i,j} \frac{|\langle j|p|i\rangle|^2}{\omega_j - \omega_i} \delta\left[\omega - (\omega_j - \omega_i)\right]$. If we assume that the dipole matrix element is independent of frequency and $\omega_j - \omega_i \approx \Delta$, we have $\alpha(\omega) \propto \sum_{i,j} \delta\left[\omega - (\omega_j - \omega_i)\right] = \sqrt{\omega - \Delta}$. Therefore, the Au55 nanoparticle behaves like a 3D semimetal with a gap Δ rather than a giant atom. Nevertheless, the robustness of the absorption edge at ~ 10 cm^{-1} with the temperature change is puzzling considering the fact that the thermal energy $k_B T \sim 0.02\, eV$ at room temperature is more than sufficient to broaden the absorption edge.

In summary, we have found that the far-IR energy gap is surprisingly small and that the frequency dependence of the absorption is completely different from that of the classical prediction calculated from the induced electric dipole absorption. The surprisingly small far-IR energy may be understood as a result of the red-shift by $\sim 0.15\, eV$ from the expected absorption due to the Coulomb energy difference involved in the transition from a doubly occupied state to a singly occupied state. The $\alpha \propto \sqrt{\omega - \Delta}$ suggests that Au55 nanoparticle may described as a 3D semimetal with an energy gap Δ. The Coulomb correlation energy difference $(U_1 - U_0)$ makes

the far-IR energy gap much smaller than the Kubo gap. We found that the absorption onset at ~ 1.2 *meV* is independent of temperature and no indication of the level correlation effect predicted by GE [4]. We anticipate that the far-IR absorption in the quantum regime will eventually recover the classical behavior at higher frequencies, which remains to be seen.

Acknowledgment:

We thank Professor Al Sievers for pointing us to Ref. 10, Professor Bruce Ault for helpful discussions on Teflon modes, and Dr. Larry Carr for making the far-IR transmission measurements on f = 0.004 Au55/Teflon sample in the magnetic field.

References

1. See *Condensed-Matter and Materials Physics: The Science of the World Around Us*, The National Academies Press (2007).

2. The term metal "nanoparticle" used in this paper is also commonly called as metal clusters, metal colloids, or small metal particles in the literature.

3. R. Kubo, *J. Phys. Soc. Jpn*. **17**, 975 (1962).

4. L.P. Gor'kov and G.M. Eliashberg, *Sov. Phys*. JETP **21**, 940 (1965). See also S. Strässler, M.J. Rice, and P. Wyder, *Phys. Rev.* B**6**, 2575 (1972) for corrections.

5. E.P. Wigner, *Ann. Math*. **53**, 35 (1951); **62**, 548 (1955).

6. F.J. Dyson, *J. Math. Phys*. **3**, 140, 166 (1962); M.L. Mehta and F.J. Dyson, *J. Math. Phys*. **4**, 713 (1963).

7. R.P. Devaty and A.J. Sievers, *Phys. Rev*. B**22**, 2123 (1980).

8. Günter Schmid, *Chem. Soc. Rev*. **37**, 1909 (2008) and references therein.

9. The temperature dependence seen between 300 K and 200 K data is due to the temperature dependence of the Teflon matrix.

10. G.W. Chantry, J.W. Fleming, E.A. Nicol, H.A. Willis, M.E.A. Cudby, and F.J. Boerio, *Polymer* **15**, 69 (1974).

11. In the low frequency limit, the energy loss due to the magnetic dipole also contributes. However, for the size of Au55, the magnetic dipole term may be ignored as its contribution becomes much smaller than that of the electric dipole. For a review, see G.L. Carr, S. Perkowitz, and D.B. Tanner, in *Infrared and Millimeter Waves*, Vol. 13, edited by Kenneth J. Button (Academic Press, Orlando, 1985) pp. 171–263 and references therein.

12. H. Zhang, G. Schmid, and U. Hartmann, *Nano Lett*. **3**, 305 (2003).

13. L. Yi and P. Sheng, *Solid State Commun*. **114**, 177 (2000).

14. G.L. Carr, private communication.

Figure Captions:

Figure 1. Models of $Au_{55}(PPh_3)_{12}Cl_6$ nanoparticle (Top) and energy level diagram of a sphere of a = 5.3 Å (Bottom).

Figure 2. Far-infrared transmission of d = 0.363 cm thick f = 0.01 Au55 in Teflon measured with three different beam splitters at temperatures 10, 20, 30, 50, 70, 100, 200, and 300 K. Note that the data are displayed as taken and not merged together. The dotted curves are taken at 300 K. Inset: Far-infrared transmission spectra of pure Teflon pellet (d = 0.373 cm) at various temperatures (see the text for details).

Figure 3. (a) Far-infrared absorption coefficient of f = 0.01 Au55 and (b) that of f = 0.01 PPh_3 ligand molecules after subtracting the Teflon background absorption. Note that the T_3 mode was not fully subtracted while the contributions of the T_1 and T_2 modes were essentially eliminated. Note also the presence of the modes denoted as L_1 and L_2 due to the PPh_3 ligand molecules. Inset: α/f vesus frequency plot (see the text for discussion).

Figure 4 Direct comparison of the measured far-infrared absorption coefficient of f = 0.01 Au55 with the calculated absorption coefficient of f = 0.01 classical Au particles of a = 5.3 Å (dashed curve).

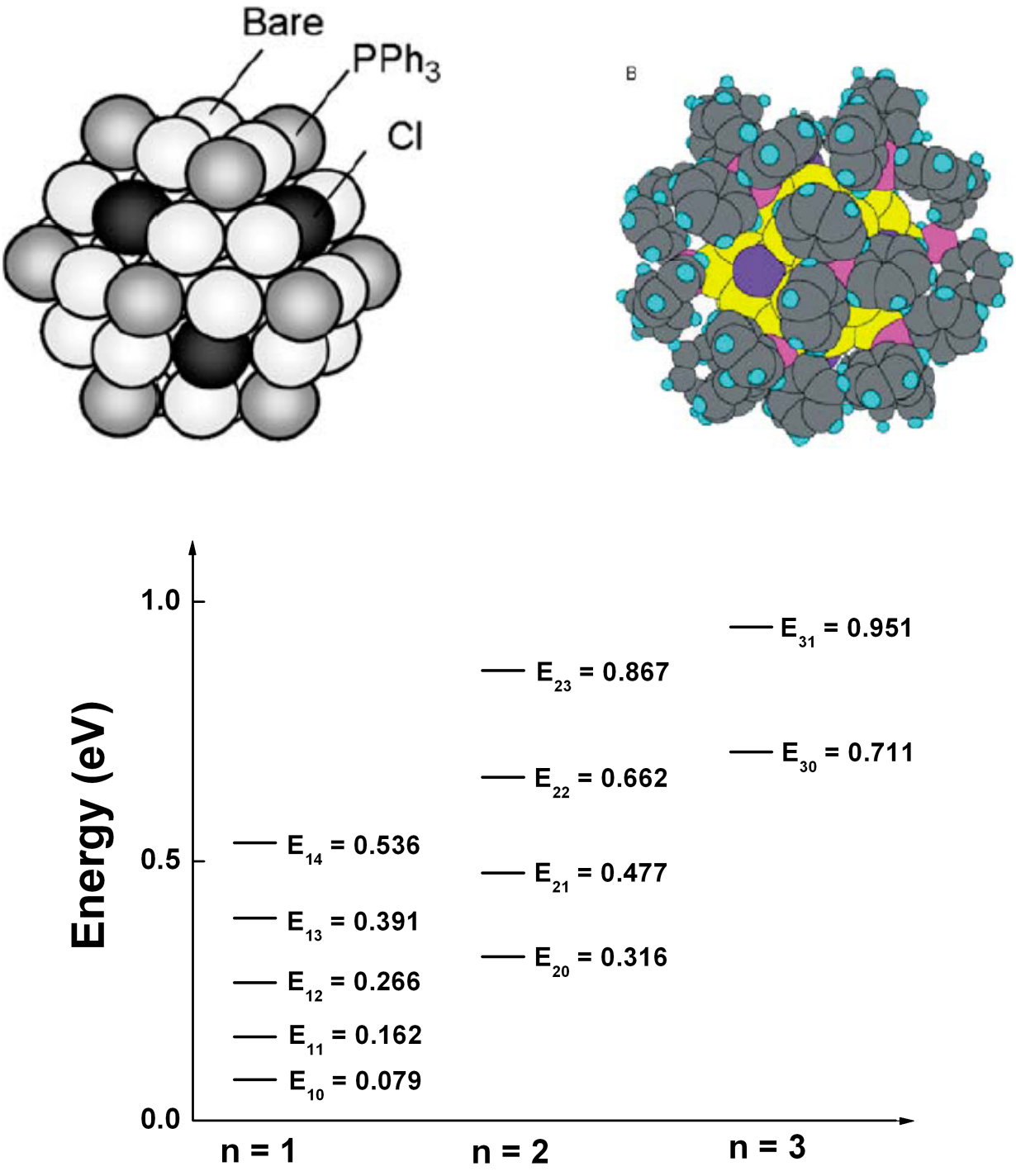
Bare
PPh3
Cl
B
Energy (eV)
1.0
0.5
0.0
E31 = 0.951
E23 = 0.867
E30 = 0.711
E22 = 0.662
E14 = 0.536
E21 = 0.477
E13 = 0.391
E20 = 0.316
E12 = 0.266
E11 = 0.162
E10 = 0.079
n = 1
n = 2
n = 3

Figure 1

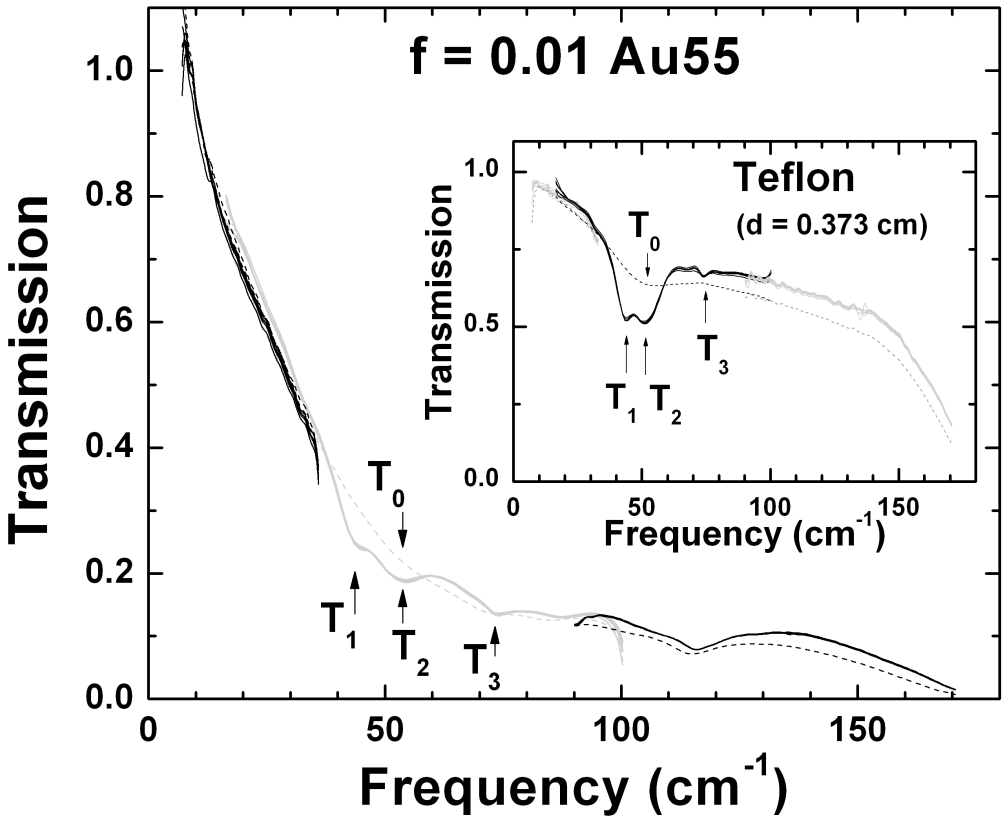
f = 0.01 Au55
Transmission
Frequency (cm-1)
T0
T1
T2
T3
Teflon
(d = 0.373 cm)
Transmission
Frequency (cm-1)
T0
T1
T2
T3

Figure 2

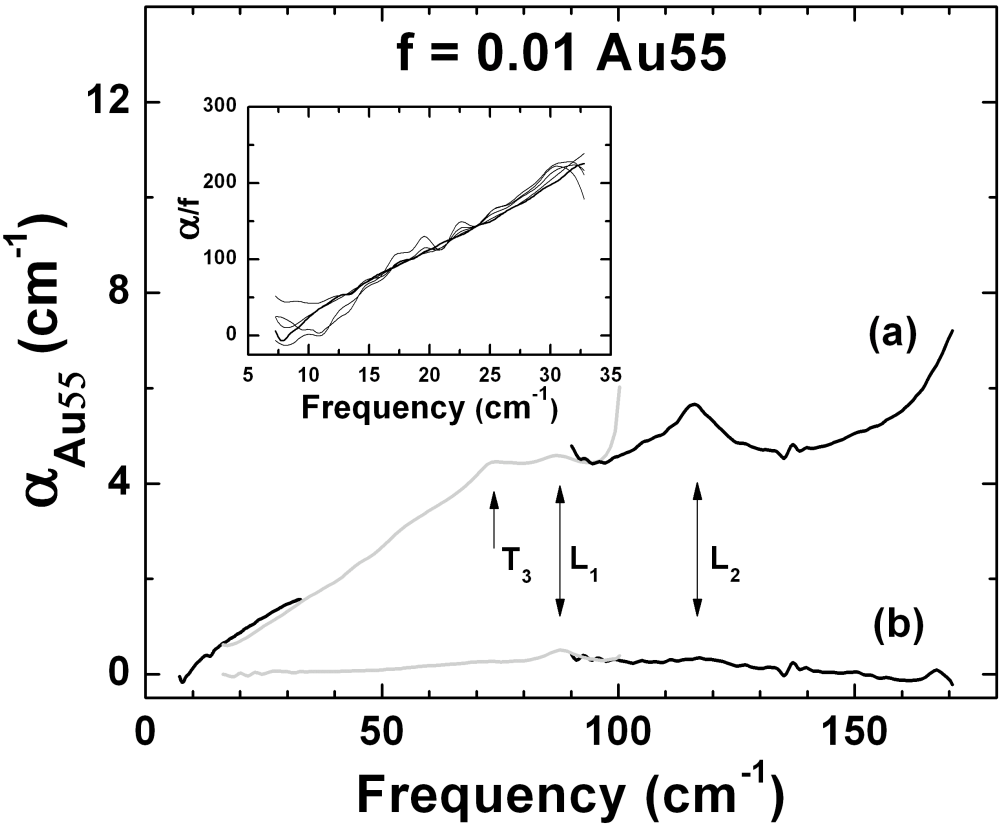
f = 0.01 Au55
α Au55 (cm-1)
Frequency (cm-1)
α/f
Frequency (cm-1)
(a)
(b)
T3
L1
L2

Figure 3

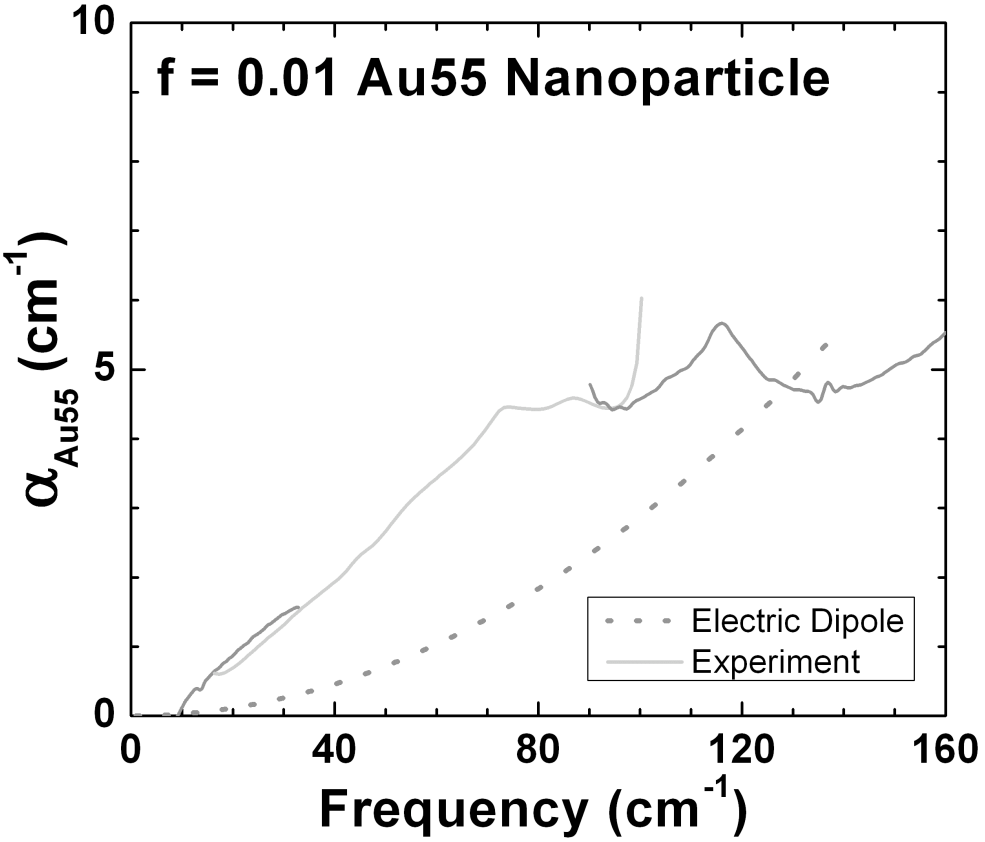
f = 0.01 Au55 Nanoparticle
α_{Au55} (cm^{-1})
Frequency (cm^{-1})
Electric Dipole
Experiment
0
5
10
0
40
80
120
160

Figure 4